An Efficient Algorithm for the Parameter Extraction of 3-D Interconnect Structures in the VLSI Circuits: Domain-Decomposition Method

Zhenhai Zhu, Hao Ji, and Wei Hong, *Member, IEEE*

***Abstract*— In this paper, the domain-decomposition method (DDM) has been used to extract the capacitance matrices of multilayered three-dimensional (3-D) interconnects in very-large-scale integration (VLSI) circuits. Different subdomains are analyzed separately, so the most efficient method can be chosen for every subdomain. Therefore, the DDM can greatly reduce the algorithm complexity and provide a good platform for the development of combining methods. Numerical results show that the computing time and memory size used by the DDM are more than ten times less than those used by Ansoft's Maxwell SpiceLink—and more importantly, they are unrelated to the thickness of the pure dielectric layers.**

***Index Terms*—Domain decomposition method, numerical methods, parameter extraction.**

I. Introduction

THE TREND of future very-large-scale integration (VLSI) circuits is toward narrower linewidth, larger die size, greater number of interconnect layers, and higher clock frequencies. As a result, the electrical characteristics of the interconnects are becoming more important factors dominating the behavior of the integrated circuits. This has increased the interest in the efficient methods for the parameter extraction.

Many numerical methods have been used to calculate the capacitance matrices of interconnects [1]–[8]. Recently, a novel algorithm called dimension-reduction technique (DRT) is developed to calculate the capacitance matrices of three-dimensional (3-D) interconnections [9], [10]. The DRT uses magnetic walls (MW's) to cut the complex interconnect net into many simple cells. By taking advantage of the known eigenmode functions in such layers as pure dielectric layers, and layers with parallel signal lines, the computing time and memory needs are reduced dramatically. However, the DRT is basically a field-matching method, so the computing time increases quadratically with the increase of the number of eigenmode functions. Therefore, when the number of conductors in one layer is large, the advantage gained from the analytical form of eigenmode functions will be completely offset by the time consumed for the inverse of large full matrices. The major source that degrades the efficiency of the DRT is that the DRT solves the Laplace equation simultaneously in every layer.

To overcome this problem, the domain-decomposition method (DDM), an efficient technique to solve the partial differential equation (PDE) [11], [12], is used to calculate the capacitance matrices of various two-dimensional (2-D) and 3-D interconnect structures. The cutting strategy in the DRT is still adopted. The DDM then decomposes each cell into subregions and separately solves the PDE in each subregion. The DDM has the following attractive features.

1) Every subregion is analyzed separately. Therefore, one can choose the most efficient method for each subregion independently. This has greatly reduced the algorithm complexity and has laid a good ground for the development of combining methods.
2) Like the DRT, many subregions, such as the subregions with the pure dielectric layers, can be analyzed analytically. Therefore, the domains that have to be analyzed numerically are reduced to the least. This has dramatically reduced memory needs and computing time, and more importantly, has made them unrelated to the thickness of the pure dielectric layers.
3) If one uses the finite-difference method (FDM) or finite-element method (FEM) to analyze subregions, the resultant sparse matrix will be much smaller than that resulted from dividing the entire region into meshes.

The sparse matrix solver takes $O(n^2)$ time for the direct methods (like LU decomposition and Gauss elimination) and $O(n^\alpha)$ time for the iterative methods [like the conjugate gradient method (CGM)], where $1 < \alpha < 2$. Thus, the central processing unit (CPU) time used for every subregion is far less than that used for the entire region. This benefit may be offset by the fact that the DDM is an iterative method, but the CPU time of the DDM will still be less than that of the traditional FEM or FDM if the iteration times are few. This advantage will be even greater if the interconnect structure has many dielectric layers and conductors.

The DDM has been used to extract the capacitance matrices of several 2-D and 3-D interconnect structures. The results are in good agreement with those of SpiceLink, but the memory size and computing time used by DDM are more than ten times less than those used by SpiceLink.

In Section II, a brief introduction of the relaxation Schwarz alternating method will be presented. The DDM for the

Manuscript received June 28, 1996; revised April 25, 1997. This work was supported by China NSF under Contract 69625102.

The authors are with the State Key Laboratory of Millimeter Waves, Department of Radio Engineering, Southeast University, Nanjing 210096, China.

Publisher Item Identifier S 0018-9480(97)05372-6.

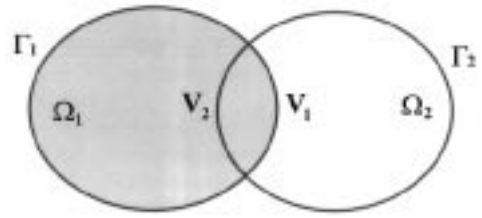

Fig. 1. Two overlapping subregions.

multilayered structures is then presented in Section III. In Section IV, several examples are given to demonstrate the flexibility and efficiency of the DDM, while conclusions are stated in Section V.

II. Relaxation Schwarz Alternating Method

There are two kinds of DDM's. For one of them, the domain is decomposed into nonoverlapping subdomains; the solution on the neighboring subdomains are related by certain continuity conditions at the interfaces. For the other kind, the domain is decomposed into overlapping subdomains, and an iterative solution procedure is used alternatively over the subdomains. The latter is usually called the Schwarz alternating method.

Consider a 3-D Dirichlet problem

$$\begin{cases} \nabla^2 u = \frac{\partial^2 u}{\partial x^2} + \frac{\partial^2 u}{\partial y^2} + \frac{\partial^2 u}{\partial z^2} = 0, & (x,y,z) \in \Omega \\ u|_\Gamma = g(x,y,z) \end{cases} \tag{1}$$

where $\Omega \in R^3$ is a bounded open region, and its boundary is Γ. Region Ω can be divided into two overlapping subregions Ω_1 and Ω_2, as shown in Fig. 1. Denoting Γ_j and V_j as the boundaries and fictitious boundaries of $\Omega_j\,(j = 1,2)$, the Schwarz alternating method can then be expressed as in the following iterative scheme:

$$\begin{cases} \nabla^2 u_1^{i+1} = 0, & (x,y,z) \in \Omega_1 \\ u_1^{i+1} = u_2^i, & (x,y,z) \in V_1 \\ u_1^{i+1} = g(x,y,z), & (x,y,z) \in \Gamma_1 - V_1 \end{cases} \tag{2}$$

$$\begin{cases} \nabla^2 u_2^{i+1} = 0, & (x,y,z) \in \Omega_2 \\ u_2^{i+1} = u_1^{i+1}, & (x,y,z) \in V_2 \\ u_2^{i+1} = g(x,y,z), & (x,y,z) \in \Gamma_2 - V_2 \end{cases} \tag{3}$$

$$i = 0,1,2,\cdots$$

where u^0 is the initial guess. A relaxation factor w can be introduced into (2), (3) to accelerate the convergence. The new scheme with the relaxation factor is

$$\begin{cases} \nabla^2 \tilde{u}_1^{i+1} = 0, & (x,y,z) \in \Omega_1 \\ \tilde{u}_1^{i+1} = u_2^i, & (x,y,z) \in V_1 \\ \tilde{u}_1^{i+1} = g(x,y,z), & (x,y,z) \in \Gamma_1 - V_1 \\ u_1^{i+1} = \tilde{u}_1^{i+1} + w_1\left(\tilde{u}_1^{i+1} - u_1^i\right) \end{cases} \tag{4}$$

$$\begin{cases} \nabla^2 \tilde{u}_2^{i+1} = 0, & (x,y,z) \in \Omega_2 \\ \tilde{u}_2^{i+1} = u_1^{i+1}, & (x,y,z) \in V_2 \\ \tilde{u}_2^{i+1} = g(x,y,z), & (x,y,z) \in \Gamma_2 - V_2 \\ u_2^{i+1} = \tilde{u}_2^{i+1} + w_2\left(\tilde{u}_2^{i+1} - u_2^i\right). \end{cases} \tag{5}$$

If $w_j \in (0,2), j = 1,2$ then for any initial guess u^0, the relaxation Schwarz alternating method converges [13]. The algorithm in (4), (5) is also valid if the region Ω is divided into more than two subregions.

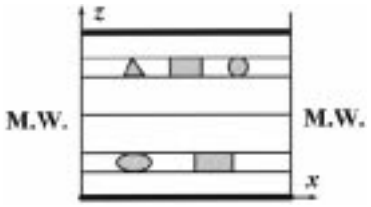

(a)

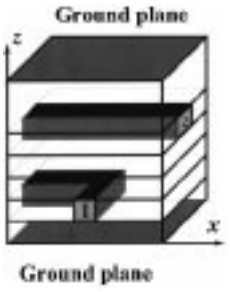

(b)

Fig. 2. Multilayered-interconnect structures. (a) Multiconductor lines. (b) One straight line over one bend.

It is obvious that the convergence rate of the Schwarz alternating method is closely related to the size of the overlapping region. A Fourier series method is used in [14], [15] to analyze the case of the rectangular subregions. The conclusion is that the iteration error decreases exponentially with the increase of the ratio of the overlapping domain over the subregion. This conclusion is extended to the general cases of arbitrary subregions in [14]. However, increase in the size of the overlapping domain will result in the increase in the computational complexity of the subregion. Hence, there exists a balance between the convergence rate and the size of the overlapping domain.

III. Domain-Decomposition Method for Multilayered-Interconnect Structures

Up to now, the effective frequency range of the signals in the VLSI system is still below 10 GHz. Therefore, the quasi-static assumption is still valid. According to the assumption, the planes, which are far enough from the signal lines or discontinuities in Fig. 2 and normal or parallel to the axis of the signal lines, can be replaced by MW's. The validation of this argument is presented in [10].

The cross section of multilayered multiconductor lines and a straight line over a bend embedded in multilayered media are shown in Fig. 2. The layers in these structures can simply be categorized into two kinds: layers with conductors and pure dielectric layers. Thus, an obvious way of decomposing the whole structure into subregions is to take a cascade of pure dielectric layers as a subregion and every layer with conductors as a subregion. For example, the domain decomposition of the structure in Fig. 2(b) is shown in Fig. 3.

A. Iteration Algorithm

Since the neighboring subregions of every subregion do not overlap, it is straightforward to extend the iteration scheme

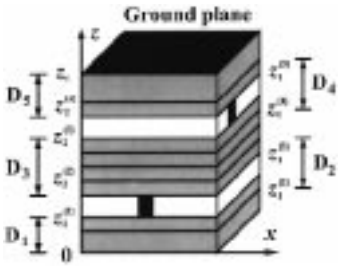

Fig. 3. Domain decomposition of the multilayered structure in Fig. 2(b).

(4), (5) for two subregions to the more general scheme for the multilayered structure with more than two subregions. Denote the upper and lower fictitious boundaries of subregion D_j as $\Gamma_2^{(j)}$: $z = z_2^{(j)}$ and $\Gamma_1^{(j)}$: $z = z_1^{(j)}$, and denote the potentials on them for the ith system iteration as $U_2^{i(j)}$ and $U_1^{i(j)}$, then in every subregion, (1) can be rewritten as

$$\begin{cases} \nabla^2 u^{(j)} = 0, & (x,y,z) \in D_j \\ \frac{\partial}{\partial n} u^{(j)}|_{\partial\Omega_j} = 0, & j = 1,2,\cdots,N_D \end{cases} \tag{6}$$

$$u^{(j)}|_{\Gamma_1^{(j)}} = U_1^{i(j)}, \qquad j = 2,3,\cdots,N_D \tag{7}$$

$$u^{(j)}|_{\Gamma_2^{(j)}} = U_2^{i(j)}, \qquad j = 2,3,\cdots,N_D - 1 \tag{8}$$

$$u^{(1)}|_{z=0} = 0 \tag{9}$$

$$u^{(N_D)}|_{z=z_t} = 0, \qquad i = 0,1,2,\cdots \tag{10}$$

where N_D is the number of the subregions, $z = z_t$ is the top plane of the subregion D_{ND}, $\partial\Omega_j$ stands for the MW's surrounding the jth subregion and $\vec{n}$ stands for the unit vector normal to $\partial\Omega_j$. After solving (6)–(10) in every subregion, the potentials on the fictitious boundaries are

$$U_1^{(j)} = u^{(j-1)}|_{\Gamma_1^{(j)}} \tag{11}$$

$$U_2^{(j)} = u^{(j+1)}|_{\Gamma_2^{(j)}}. \tag{12}$$

Using the relaxation iterative scheme

$$U_k^{i+1(j)} = U_k^{i(j)} + w_j\big(U_k^{i(j)} - U_k^{(j)}\big), \qquad k = 1,2 \tag{13}$$

one obtains the new potentials on the fictitious boundaries for the next system iteration. Similar to (4) and (5), if $w_j \in (0,2), j = 1,2,\cdots,N_D$, then for any initial guess $U_k^{0(j)}(k = 1,2)$, the above iterative scheme converges.

The subregions can also be classified into two categories: subregion with conductors, such as D_2 and D_4 (Fig. 3) and pure dielectric subregion, such as D_1, D_3, and D_5 (Fig. 3). The subregion with pure dielectric layers is homogeneous along x- and y-directions; hence, the analytical method such as the mode-matching method (very similar to that presented in [9]–[10]) is the most suitable method. However, the subregion with conductors is generally inhomogeneous along x-, y-, and z-directions, so one has to choose a flexible and efficient method, such as the FDM, to solve (6) in this subregion. Therefore, the DDM has set up a very good platform for one to develop combining methods.

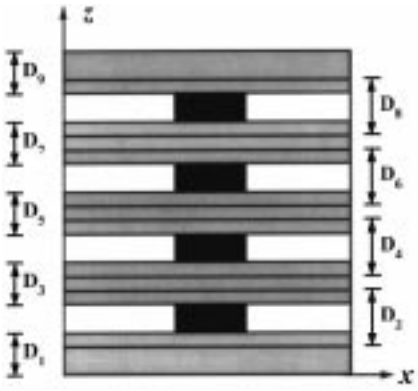

Fig. 4. Four conductors embedded in nine dielectric layers.

TABLE I
THE NUMBER OF ITERATIONS OF DIFFERENT SEQUENCES

	sequence 1	sequence 2	sequence 3
$j = 2$	13	16	13
$j = 4$	12	14	12
$j = 6$	14	12	10
$j = 8$	18	15	12
total iterations	57	57	47

B. Iteration Sequence

When using the DDM to analyze the multilayered structure, shown in Fig. 4, there are three typical iteration sequences as follows:

1) $D_1 \to D_2 \to D_3 \to D_4 \to D_5 \to D_6 \to D_7 \to D_8 \to D_9$

or

$$D_9 \to D_8 \to D_7 \to D_6 \to D_5 \to D_4 \to D_3 \to D_2 \to D_1;$$

2) $$\begin{cases} D_2 \\ D_4 \\ D_6 \\ D_8 \end{cases} \to \begin{cases} D_1 \\ D_3 \\ D_5 \\ D_7 \\ D_9 \end{cases};$$

3) $$D_j \to \begin{cases} D_{j-1} \to D_{j-2} \to \cdots \to D_1, \\ D_{j+1} \to D_{j+2} \to \cdots \to D_9, \end{cases} \qquad j = 2,4,6,8$$

where the subregions to the right of the symbol "{" can be interchanged during the iteration. These three iteration sequences have been used to analyze the structure in Fig. 4. The number of iterations is shown in Table I, from which one can see that sequence 3 is the best one. As far as is known, there is no rule about how to choose the best iteration sequence, so sequence 3 will be used throughout this paper because there is numerical evidence to support this choice.

IV. NUMERICAL RESULTS AND DISCUSSIONS

In this section, the DDM is used to analyze several 2-D and 3-D interconnect structures, and the results are compared with those of a FEM-based commercial tool, Ansoft's Maxwell SpiceLink. Since the results of the quasi-static analysis are unrelated to the units of the size of the interconnects, relative

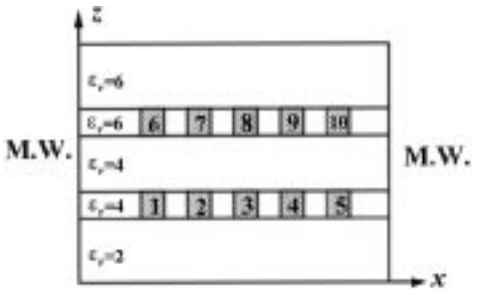

Fig. 5. Ten conductors embedded in five dielectric layers.

TABLE II
ITERATIONS VERSUS RELAXATION FACTOR

w	0.9	1.0	1.1	1.2	1.3	1.4	1.5	1.6	1.7	1.8	1.9
iterations	124	109	99	89	80	73	69	61	76	94	112

values as the size of the interconnects will be used. The convergence criteria of the DDM is

$$\max_{n=1,2}\max_{1\le j\le N_D}\frac{\left\|U_n^{i+1(j)}-U_n^{i(j)}\right\|_2}{\left\|U_n^{i+1(j)}\right\|_2}<\delta \tag{14}$$

where $\|\bullet\|_2$ stands for the Euclidean norm and δ is a user-specific threshold value. For clarity, only the diagonal elements of the capacitance matrix are presented if the number of the conductors is over five.

A. 2-D Interconnect with Ten Conductors Embedded in Five Dielectric Layers

The cross section of the interconnect is shown in Fig. 5. Ten conductors are embedded in five dielectric layers supported by a ground plane. The size of every conductor is 5×5, the gap between the conductors is 5, the thickness of every pure dielectric layer is 12. The distance between the conductor and the MW is 10. The relative dielectric constant of every layer is 2, 4, 4, 6, 6. (counted from bottom). The top layer is covered by open air.

The thickness of every overlapping region is set to be 4. The threshold value in (14) is $\delta = 1\%$. The truncated mode number in every pure dielectric layer is 10. The iterations versus relaxation factor is shown in Table II, from which one can see that the optimal relaxation factor is $w = 1.6$. As far as is known, no rules have been presented to choose the optimal relaxation factor [13]. Therefore, a trial-and-error process has to be used to decide an optimal factor for a specific structure. Fortunately, it has been found that for multilayered structures, the optimal relaxation factor is always around 1.5. Thus, 1.5 was chosen as a fixed value of the relaxation factor. The diagonal entries of the capacitance matrix calculated by the DDM and SpiceLink are compared in Table III. The discrepancy between two results is within 5%. In the Sun SPARC workstation 4, the computing time of the DDM is 15 s when $w = 1.6$, while that of the SpiceLink is 28 s. Therefore, the algorithm in this paper is both correct and efficient.

TABLE III
DIAGONAL ENTRIES OF THE CAPACITANCE MATRIX
CALCULATED BY THE DDM AND SPICELINK (IN pF/m)

	C_{11}	C_{22}	C_{33}	C_{44}	C_{55}	C_{66}	C_{77}	C_{88}	C_{99}	$C_{10,10}$
DDM	118.74	158.51	158.52	158.51	118.73	154.96	236.85	237.45	236.85	154.96
SpiceLink	118.12	152.32	152.57	151.96	117.97	152.55	233.30	233.84	231.87	152.19

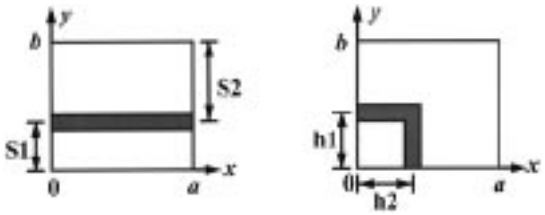

(a) (b)

Fig. 6. Top view of the layers with conductors in Fig. 2(b), $a = 9$, $b = 8$. (a) Layer with a straight line, $S1 = 3$, $S2 = 5$. (b) Layer with a bend, $h1 = h2 = 3.5$.

B. 3-D Interconnect with One Straight Line Over One Bend

The structure is shown in Fig. 2(b) and the top view of the layer with a straight line and the layer with a bend is shown in Fig. 6(a) and (b), respectively. The size of the cross section of each conductor is 1×1. Counted from the bottom, the thickness of every layer is 1, 1, 1, 1, 1, and 2, the dielectric constants are 2, 4, 4, 4, 6, and 6. Other geometrical parameters are shown in Fig. 6. The thickness of the overlapping domains are 0.5. Truncated mode numbers along x- and y-directions are 5. The optimal relaxation factor is $w = 1.5$. The threshold value in (14) is $\delta = 1\%$.

The capacitance matrices calculated by the DDM and SpiceLink are shown in (15), (16), the discrepancy between two results is within 5%. In SunSparc workstation 20, the computing time and memory size used by the DDM and the SpiceLink are 12 s and 0.588 Mbytes, 343 s and 39.1 Mbytes, respectively. Therefore, the computation sources used by SpiceLink are about 30 times those used by the DDM

$$\text{DDM: } [C] = \begin{bmatrix} 0.812 & -0.259 \\ -0.259 & 1.32 \end{bmatrix} \text{pF} \tag{15}$$

$$\text{SpiceLink: } [C] = \begin{bmatrix} 0.779 & -0.26 \\ -0.26 & 1.38 \end{bmatrix} \text{pF}. \tag{16}$$

C. Four Conductor Crossovers Above Two Bends Embedded in Seven Dielectric Layers

The structure is shown in Fig. 7. The size of every straight lines is $1 \times 1 \times 13$, the gap between conductor 3 and 4, as well as conductor 5 and 6, is 3. The distance between the straight line and MW is 4. The size of the cross section of every bend is 1×1, other geometric parameters of the bends are shown in Fig. 8. Counted from the bottom, the thickness of every dielectric layer is 1, 1, 2, 1, 1, 1, and 1,

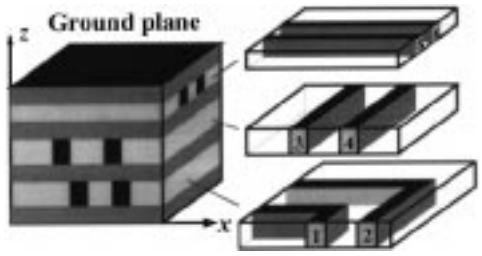

Fig. 7. Crossovers above bends embedded in seven dielectric layers.

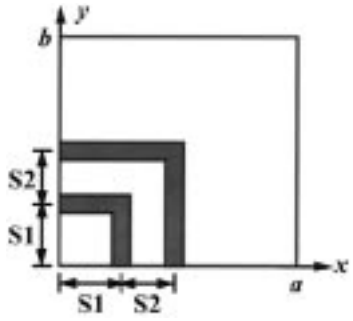

Fig. 8. Top view of the layer with bends in Fig. 7, $a = b = 13$, $S1 = 3.5$, $S2 = 3$.

TABLE IV
DIAGONAL ENTRIES OF THE CAPACITANCE MATRICES (IN pF)

	C_{11}	C_{22}	C_{33}	C_{44}	C_{55}	C_{66}
DDM	0.680	1.29	1.57	1.52	2.54	2.54
SpiceLink	0.669	1.29	1.60	1.54	2.53	2.53

the dielectric constant of every layer is 2, 3, 3, 4, 4, 5, and 5. The thickness of the overlapping domain is 0.5, the truncated mode numbers along x- and y-directions in each pure dielectric subregion are 5, the optimal relaxation factor is $w = 1.5$, the threshold value in (14) is $\delta = 1\%$. The capacitance matrices calculated by the DDM and SpiceLink are compared in Table IV, the discrepancy of two results is within 2%. In Sun SPARC workstation 20, the computing time and memory size used by the DDM and the SpiceLink are 122 s and 2.7 Mbytes, 1327 s and 75.9 Mbytes, respectively. Therefore, the computation sources used by SpiceLink are more than ten times those used by DDM.

Since every subregion is analyzed separately, the algorithm complexity is reduced dramatically. For instance, to analyze the structure in Fig. 7, only three independent codes for the basic subregions are needed. They are: 1) the code for the subregion with single-layered bends; 2) the code for the subregion with single-layered straight lines; and 3) the code for the pure dielectric subregion. The size and complexity of each subregion is much smaller than those of the whole structure; hence, every code is much simpler than that for the analysis of the whole structure. Using these three codes, many kinds of combining structures can be analyzed, such as the structures in Figs. 2(b) and 7. The number of basic subregions is limited, so if a library is set up consisting of the independent subroutines for these basic subregions, then based upon the DDM, this library can be used to analyze most interconnect structures in VLSI circuits.

V. CONCLUSION

In this paper, the DDM has been used to calculate the capacitance matrices of 2-D and 3-D multilayered-interconnect structures in VLSI circuits. Numerical results show that the computing time and memory used by Ansoft's SpiceLink are more than ten times those used by the DDM. Aside from this, the memory needs and computing time of the DDM are unrelated to the thickness of the pure dielectric layers. The DDM provides a good platform for the development of combining methods and a good framework for the development CAD software for the interconnect problems.

REFERENCES

[1] T. Chou and Z. J. Cendes, "Capacitance calculation of IC packages using the finite element method and planes of symmetry," *IEEE Trans. Computer Aided Design*, vol. 13, pp. 1159–1166, Sept. 1994.

[2] M. Naghed and I. Wolff, "Equivalent capacitances of coplanar waveguide discontinuities and interdigitated capacitors using a 3-D finite difference method," *IEEE Trans. Microwave Theory Tech.*, vol. 38, pp. 1808–1815, Dec. 1990.

[3] W. Hong, W. K. Sun, and W. W. M. Dai, "Fast parameter extraction of multilayer and multiconductor interconnects using geometry independent measured equation of invariance," in *IEEE MCMC*, Santa Cruz, CA, Feb. 1996, pp. 105–110

[4] Z. Zhu, W. Hong, Y. Y. Chen, and Y. Y. Wang, "Electromagnetic modeling and transient simulation of interconnects in high speed VLSI circuits," *Proc. Inst. Elect. Eng.*, vol. 143, no. 5, pt. H, pp. 373–378, Oct. 1996.

[5] C. Wei and R. F. Harrington, J. R. Maurtz, and T. K. Sarkar, "Multiconductor transmission lines in multilayered dielectric media," *IEEE Trans. Microwave Theory Tech.*, vol. MTT-32, pp. 439–449, Apr. 1984.

[6] K. S. Oh, D. Kuznetsov, and J. E. Schutt-Aine, "Capacitance computations in a multilayered dielectric medium using closed-form spatial green's functions," *IEEE Trans. Microwave Theory Tech.*, vol. 42, pp. 1443–1453, Aug. 1994.

[7] R. Wu, "Resistance computations for multilayer packaging structures by applying the boundary element method," *IEEE Trans. Comp. Packag. Hybrids, Manufact. Technol.*, vol. 15, pp. 87–95, Jan. 1992.

[8] K. Nabors and J. White, "Multipole-accelerated capacitance extraction algorithms for 3-D structures with multiple dielectrics," *IEEE Trans. Circuits Syst.*, vol. 39, pp. 946–954, Nov. 1992.

[9] W. Hong, W. Sun, Z. Zhu, H. Ji, B. Song, and W. W. M. Dai, "A novel dimension reduction technique for the capacitance extraction of 3-D VLSI interconnects," in *IEEE/ACM Int. Conf. Comput.-Aided Design*, San Jose, CA, Nov. 1996, pp. 381–385.

[10] ———, "A novel dimension reduction technique for the capacitance extraction of 3-D VLSI interconnects," *IEEE Trans. Microwave Theory Tech.*, to be published.

[11] T. F. Chan, R. Glowinski, J. Periaux, and D. B. Widlund, Eds., *Domain Decomposition Methods*. Philadelphia, PA: SIAM, 1989.

[12] R. Glowinski, G. H. Golub, G. A. Meurant, and J. Periaux, Eds., *Proc. 1st Int. Symp. Domain Decomposition Method for Partial Differential Equations SIAM*, Philadelphia, PA, 1988

[13] W. Han, "A note on a relaxation Schwarz alternating method," *J. Comput. Appl. Math.*, vol. 34, pp. 125–130, 1991.

[14] T. Lu, J. Shi, and Z. Liu, *The Domain Decomposition Method—A New Technique for Partial Differential Equations* (in Chinese). Beijing, China: Science Press, 1992.

[15] W. P. Tang, "Schwarz splitting and template operators," Ph.D. dissertation, Dept. Mathematics, Stanford Univ., Standford, CA, 1987.

Zhenhai Zhu was born in Changsha, China, on October 22, 1970. He received the B.S. and Ph.D. degrees in electric engineering from the Southeast University, Nanjing, China, in 1992, and 1997, respectively.

From 1992 to 1993, he was a Research Assistant studying scattering and radiation of electric large bodies. Between 1994 and 1997, his work was mainly focused on modeling and simulation of the 3-D VLSI interconnects embedded in multilayered medium. He has authored and co-authored over ten papers appearing in international journals and conference proceedings.

Hao Ji was born in Nanjing, China, in 1973. She received the B.S. and M.S. degrees in electrical engineering from Southeast University, Nanjing, China, in 1994 and 1997, respectively.

Her current research interests include computational electromagnetic field and parameter extraction of interconnects in VLSI and MCM.

Wei Hong (M'92) received the B.S. degree from the Zhenzhou Institute of Technology, Zhenzhou, China, in 1982, and the M.S. and Ph.D. degrees from the Southeast University, Nanjing, China, in 1985 and 1988, respectively, all in electrical engineering.

Since 1988, he has been with the State Key Laboratory of Millimeter Waves, Southeast University, and is currently a Professor, Associate Dean of the Department of Radio Engineering, and Director of the Electromagnetic and Microwave Laboratory. In 1993 and 1995, he was a Visiting Scholar with the University of California at Berkeley and at Santa Cruz, respectively. His research interests include numerical methods for electromagnetic problems, millimeter-wave theory and technology, antennas, electromagnetic scattering and propagation, RF front-end for mobile communications, and the parameters extraction of interconnects in VLSI circuits. He has authored and co-authored over 130 technical publications, including his book *Principle and Application of the Method of Lines*.

Dr. Hong was awarded the first-class Science and Technology Progress Prizes issued by the State Education Commission, in 1992 and 1994, respectively, due to his research work on the functional methods and the method of lines for electromagnetic-field boundary-value problems, and in 1991, was awarded both the fourth-class National Natural Science Prize, due to his study on the numerical analysis of millimeter-wave passive circuits, and the third-class Science and Technology Progress Prize of Jiangshu Province, due to his development of millimeter wave oscillators. He is recipient of the Trans-Century Training Program Foundation for the Talents and the award of Distinguished China Doctorate Recipients, both issued by the State Education Commission, and has been recognized by the National Foundation for Distinguished Young Investigators.